Discover Mechanical Engineering

Discover

Research

An investigation on the mechanical behaviour of sandwich composite structures with circular honeycomb bamboo core

Lívia Ávila de Oliveira[1,2] · Matheus Milagres Vieira[1] · Júlio Cesar dos Santos[1] · Rodrigo Teixeira Santos Freire[1,2] · Maikson Luiz Passaia Tonatto[3] · Túlio Hallak Panzera[1,2] · Pedram Zamani[4] · Fabrizio Scarpa[5]

Received: 20 October 2022 / Accepted: 23 November 2022
Published online: 05 December 2022

Abstract
Sandwich panels made with a bamboo core of different dimensions, packing geometries and facing materials are subjected to three-point bending tests and assessed through statistical and failure analysis. In addition to promoting a circular economy, this architecture holds great promise for replacing secondary structural components in sustainable construction and transportation facilities. The statistical analysis responses are associated with the equivalent density of the panels, flexural strength and modulus of the panels, skin stress and core shear strength and modulus. Individual bamboo rings are also characterised using physic mechanical and interfacial bonding tests. Treated aluminium face sheets provide the best mechanical performance compared to glass fibre-reinforced composite (GFRP) ones by increasing the overall properties of the sandwich panels. The specific face sheet material and void percentage affect the equivalent density, with lower values (~ 0.48 g/cm^3) when using GFRP skins, larger bamboo rings and cubic packing. Sandwich panels with 30 mm bamboo rings and hexagonal packing provide higher flexural properties, i.e. ~ 43 MPa strength and ~ 7.6 GPa modulus, and skin stress (~ 288 MPa), while those with 20 mm bamboo rings have higher shear stiffness (~ 132 MPa) and resistance (~ 3.33 MPa). Sandwich panels made with aluminium skins show evident skin-polymer debonding, while those with GFRP have premature skin failure and lower structural performance. The proposed sandwich panels present remarkable and competitive mechanical performance concerning commercial analogous structures, generally used in the aeronautical and automotive industries.

Keywords Sandwich panel · Bamboo core · Aluminium skin · GFRP skin · Flexural properties · Lap shear testing · Green composite structure · Statistical analysis · Design of experiment

1 Introduction

Sandwich panels are typically made of two thin skin sheets and a core material of comparatively higher thickness and lower density [1, 2]. The outer skins are usually designed to withstand axial and bending loads, while the core material resists shear [2]. The sandwich panels combine lightweight characteristics with high stiffness and strength, resulting in excellent mechanical performance and structural efficiency [3]. These characteristics have led to increased

✉ Túlio Hallak Panzera, panzera@ufsj.edu.br | [1]Centre for Innovation and Technology in Composite Materials—CITeC, Department of Mechanical Engineering, Federal University of São João del Rei-UFSJ, Praça Frei Orlando, 170, São João del Rei 36307-352, Brazil. [2]Department of Natural Sciences, Federal University of São João del Rei-UFSJ, São João del Rei, Brazil. [3]Department of Mechanical Engineering, Federal University of Santa Maria-UFSM, Santa Maria, Brazil. [4]Department of Mechanical Engineering, Faculty of Engineering, Ferdowsi University of Mashhad, Mashhad, Iran. [5]Bristol Composites Institute, University of Bristol, Bristol BS8 1TR, UK.

demand for those panels to build roofs, sports equipment, and engineering structures such as automotive bodies, wind turbine blades, aerospace structures, marine components, high-speed railways, and other applications [4–7].

A wide variety of materials is used for skins, ranging from metals such as aluminium [8] and steel [9], to non-metals, such as polymeric composites reinforced with carbon [10], glass [11], natural [12] and mineral fibres [13], plywood [14] and others [15]. The core type classification can be performed from either material type or core-geometry aspects [16, 17]. For instance, the core of a sandwich composite can consist of polymeric [18] and metallic [19] foams, while, regarding the application and philosophy of structural design, it can be of honeycomb, corrugated [20], lattice, and bio-inspired geometries [21–25].

It is possible to obtain different sets of properties and target performances by varying the core material/shape, thickness, and outer face sheet material in sandwich structures [26]. Therefore, the optimal design of sandwich structures has been a challenging engineering problem for a long time [27]. Another demand faced by researchers is to design new high-performance products without compromising the availability of resources for future generations. The scientific community has recently made considerable efforts to develop sustainable and high-quality sandwich panels using alternative materials from biodegradable resources with the goal of carbon neutrality [28–33]. Recent government laws concerning greenhouse gas emissions encourage engineers and researchers in the automotive industries to produce fuel-efficient materials, replacing internal and external metal parts with lightweight green materials to improve fuel consumption and reduce emissions [32].

Bamboo is an abundant natural composite in tropical regions such as South America and Asia. This natural composite material has gained popularity within the green technology community because of its environmentally beneficial characteristics, such as renewability, biodegradability, versatility and fast growth [34–36]. Due to the high strength-to-weight ratio, bamboo can be a suitable alternative to traditional structural materials such as steel and aluminium alloys for structural applications [37–39].

The geometry of bamboo consists of a hollow quasi-cylindrical structure periodically divided by diaphragms [40]. Accordingly, in recent years, some research works were focused on the application and performance of bamboo materials as the green circular core of sandwich composites. Darzi et al. [41–43] performed numerical and experimental studies on sandwich panels made of plywood faces and bamboo ring cores. The bamboo core sandwich (BCS) was tested under flexural, shear and compressive loads. Results showed that BCSs provide superior performance, approximately 27.3%, under combined axial and bending loading compared to similar size cross-laminated timber (CLT). Compared to CLTs, bamboo sandwich structures also possess a reduced weight, lower material costs, ease of manufacture, and use of sustainable/waste products. Hartoni et al. [44] evaluated the effect of core and skin thickness of sandwich panels made of plywood faces and bamboo rings core under three-point bending tests. The results showed that the flexural strength of the sandwich composite is affected by different effects of the thickness of the core and the skin. The highest flexural strength was achieved when the core/skin thickness ratio was one. The sandwich structure with a thickness of 70–60 mm obtained increases in bending strength of 61.05% compared to the sandwich panels of 50–90 mm (core-skin).

Oliveira et al. [45] investigated the bending and shear properties of sandwich panels, including bamboo core and prepreg flaxtape skins, by varying the bamboo diameter and the adhesive type. They concluded that the core cell dimensions significantly affect the flexural and shear properties of the panels, while the physical and mechanical characteristics of the adhesives directly affect the failure mode and the overall structural integrity of the panels. Oliveira et al. [46] reported the mechanical performance of sandwich panels made of aluminium skins and Ø30 and Ø45 mm bamboo rings, achieving an enhanced behaviour when using smaller diameter rings. More recently [47], sandwich panels composed of Ø20 and Ø30 mm bamboo rings, aluminium skins and biobased adhesive were tested in a drop tower impact test. Both rings achieved equivalent dynamic behaviour.

These recent research studies have shown that sandwich panels made from a bamboo ring core could provide a feasible and promising potential for future sustainable engineering structures [45–47]. However, systematic research is still needed to improve the knowledge about the influence of various parameters on the mechanical behaviour of sandwich panels, including green materials as the core and face sheet segments. This improvement in the circle of knowledge can significantly help structural engineers to achieve a design strategy to introduce a more efficient and cost-effective sandwich composite structure. The present work is focused on evaluating the mechanical performance of sandwich panels made of bamboo rings under three-point bending as a secondary structural component in construction and transportation facilities. This is the first attempt to use glass fibre-reinforced polymers (GFRP) as facing material, widely employed in manufacturing sandwich composites. A statistical design of experiment (DoE) is performed to consider the effect of the type of material of the face skins (aluminium and GFRP), the diameter of the

bamboo rings (20 and 30 mm) and the packing geometry (hexagonal and cubic) on the flexural, shear and equivalent density of the sandwich panels. The interfacial bonding strength of the components is evaluated via single-lap joint tests. Failure of these sandwich panels is also benchmarked against analogous commercially available structures to better assess the performance of these sustainable panels for different structural applications.

2 Materials and methods

2.1 Materials

The sandwich panels are made from aeronautical aluminium of 2024-T3 grade with 0.43 mm thickness and fibre-reinforced polymer epoxy composites (GFRP) as skin materials. GFRPs made by stacking 4 layers of E-glass cross-ply are produced by hand lay-up technique followed by a vacuum bag. The corresponding thickness of GFRP is 0.65 (± 0.05) mm. The core section of these composite structures consists of treated bamboo rings which are bonded to the facesheet using an epoxy resin as the adhesive material. The GFRP is made of 200 g/m^2 cross-ply E-glass fibre fabric (supplied by Redelease, Brazil) and epoxy matrix with 5:1 resin to hardener mixing ratio by weight (Renlam M/Aradur HY956 hardener, Huntsman). The same type of epoxy polymer is used as the adhesive to bond the core section to the facesheets. Tensile, compressive and bending samples are fabricated by pouring the epoxy polymer into silicone moulds in accordance with ASTM D638 [48], ASTM D695 [49] and ASTM D790 [50], respectively. Tensile strength/modulus of 34.60 ± 0.04 MPa/2.28 ± 0.06 GPa, compressive strength/modulus of 69.55 ± 0.24 MP /2.24 ± 0.11 GPa and flexural strength/modulus of 62.26 ± 0.08 MPa/2.14 ± 0.05 GPa are obtained.

Bamboo strength and stiffness are affected by age. The literature recommends their use after at least 2 years old [51]. Bamboo culms approximately three years old belong to the *Bambusa tuldoides* species and are harvested at the Federal University of São João del-Rei (Brazil, 21°08′26.5″S 44°15′41.3″W). Boric acid (H_3BO_3, 99%) and copper sulphate ($CuSO_4.5H_2O$, 98.5%), provided by *Dinâmica Química Contemporânea Company*® (Brazil), are used for the preservative treatment of bamboo rings.

The properties of individual components (i.e., core and faces) are obtained through physical and mechanical testing. To obtain mechanical properties such as ultimate tensile strength (σ_T) and modulus of elasticity (E_T), fifteen specimens of 2024-T3 aluminium and GFRP are subjected to tensile tests following ASTM E8/E8M [52] and ASTM D3039 [53], respectively. The mechanical properties of bamboo rings, i.e., compressive elastic modulus (E_c), are obtained in quasi-static mechanical tests where the samples follow the aspect ratio of 2 to 1 for height-diameter. The test is performed on a 100 kN Shimadzu AG-X Plus testing machine (Fig. 8a, b) at 2 mm/min. The apparent density of GFRP skins (ρ_{GFRP}) is evaluated following the ASTM D792 standard [54].

2.2 Design of experiments

Statistical planning/design of experiments of the design space of the materials is performed before the start of the experimental process, which can improve the efficiency and performance of the investigation by reducing the variability, time and operating costs [55]. A full factorial design (2^3) is carried out to evaluate the effect of the face sheet material (aluminium and GFRP), core cell diameter (Ø20 and Ø30 mm) and packing geometry (hexagonal and cubic) on the mechanical behaviour of the sandwich panels. Accordingly, a total number of eight test cases, with two replicates, was conducted according to the full factorial design of experiments (Table 1). For each replicate, five samples are produced. The responses of the experiments are the equivalent density of the panels, the flexural strength and modulus, the skin stress, and the core shear modulus and stress. Design of Experiment (DoE) and Analysis of Variance (ANOVA) are performed using the Minitab v.18 software.

2.3 Specimen manufacturing

2.3.1 Skin and core preparation

GFRP skins are fabricated by vacuum lamination, with a fibre volume fraction of 60%. Four cross-ply E-glass fibre fabrics with a stacking sequence of $[0°/90°]_4$ are used to manufacture a 430 × 430 mm^2 composite plate to obtain uniform skins

Table 1 Full factorial table of experiments

E.C	Facing material	Bamboo diameter (mm)	Packing geometry	Terminology
1	Aluminium	20	Hexagonal	Al_20_Hex
2	Aluminium	20	Cubic	Al_20_Cub
3	Aluminium	30	Hexagonal	Al_30_Hex
4	Aluminium	30	Cubic	Al_30_Cub
5	GFRP	20	Hexagonal	GF_20_Hex
6	GFRP	20	Cubic	GF_20_Cub
7	GFRP	30	Hexagonal	GF_30_Hex
8	GFRP	30	Cubic	GF_30_Cub

by discarding the edges. The epoxy system (RenLam M and HY956 hardener) is hand-mixed according to the manufacturer's recommendations (with a resin-to-hardener weight ratio of 5:1), poured between the layers of fabric and spread with a spatula (Fig. 1a). The composite is sealed with a breather and release film. A vacuum pressure of 101 kPa (1 atm) is applied for 24 h (Fig. 1b). Subsequently, the composite is removed from the vacuum system and cured for seven days at room temperature (~ 25 ℃, 55%RH). Finally, the skins are cut by a band saw (Fig. 1c) and placed in a plastic bag to prevent moisture absorption until the panels are manufactured.

The 2024-T3 aluminium alloy sheets are initially cut with a guillotine (Fig. 2a) and degreased with Brazilian commercial detergent (neutral pH) under running water (Fig. 2b). The skins are then subjected to a manual mechanical abrasion using 180-grit sandpaper (Fig. 2c) along the longitudinal direction (0°) to remove the passive oxide layer and to increase the affinity with the adhesive [56]. After this process, the aluminium skins are cleaned with acetone to remove the contaminants and aluminium swarf and placed in a plastic bag until the start of sandwich panel fabrication.

Bamboo has low dimensional stability due to shrinking/swelling activity caused by loss or gain of environmental moisture due to its natural hydrophilicity. Heat treatment, for instance, can improve the quality of dimensional stability by reducing water permeability, which enhances the hydrophobicity of bamboo products [57]. In addition, due to its hydrophilicity and the natural composition of some nutrients, bamboo has less natural resistance against mould, fungi, and insects. Treatment is necessary to prevent the biological degradation of bamboo due to its high starch content through chemical modification. Wu et al. [58] reported improvement in the anti-mould capacity of bamboo through sequential chemical alkaline treatment and laccase-mediated thymol modification. However, in the present work, bamboo undergoes a protective treatment that follows the guidelines of a previous study [45]. Bamboo culms

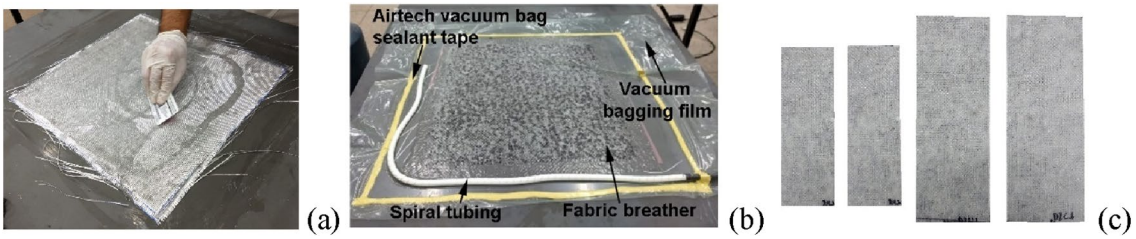

Fig. 1 GFRP skin manufacturing process: **a** Manual lamination, **b** Vacuum system and **c** GFRP skins

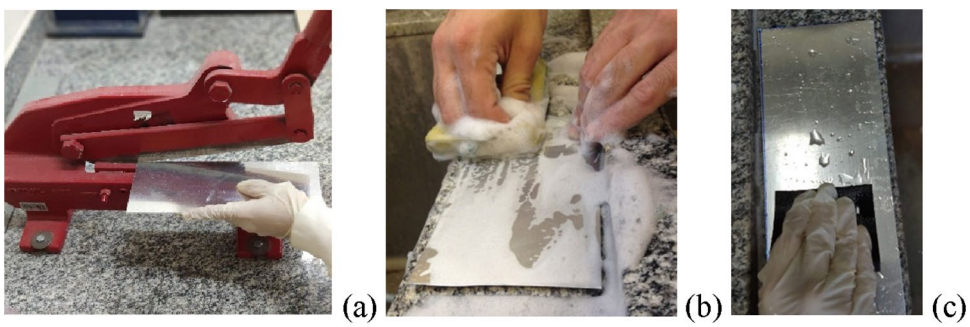

Fig. 2 Aluminium treatment: **a** cutting, **b** degreasing and **c** sanding

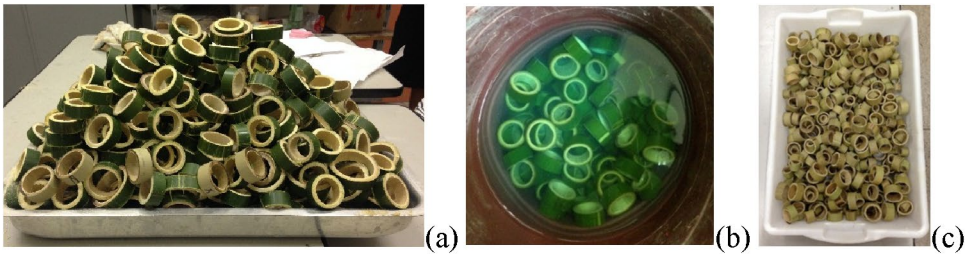

Fig. 3 Bamboo treatment process: **a** cutting the rings, **b** immersion in the solution and **c** drying [43]

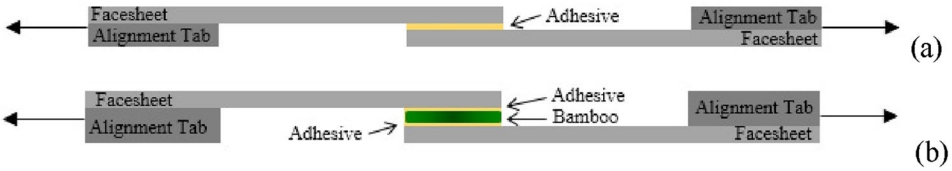

Fig. 4 Schematic of adhesion testing single lap joint specimens: **a** skin-to-polymer and **b** skin-to-polymer-to-bamboo

are harvested and left upright for two weeks to drain the starch and stabilise the shrinkage of their diameter (Fig. 3). Bamboo is weighted to constant mass over weeks. The rings are then cut according to the core cell dimensions (Ø20 and Ø30 mm, considering a maximum variation of ± 1 mm) and immersed for seven days in a preservative solution containing 3% (m/v) of boric acid and 1% (m/v) of copper sulphate. Finally, the bamboo rings are dried in an oven (ICAMO St 200) at 50 ℃ for three days.

2.4 Specimen fabrication for the adhesion tests

Prior to fabrication and evaluation of sandwich panels, single lap joint specimens are prepared as a representative testing sample to assess the interfacial adhesion strength of components such as skin-to-polymer (adhesion test I) and skin-to-polymer-to-bamboo (adhesion test II). The schematic presentation of the single lap joint specimens for adhesion testing of skin-to-polymer and skin-to-polymer-to-bamboo is shown in Fig. 4. Metal supports (the alignment tabs in Fig. 4) are used during the lap shear tests to keep the alignment in loading and prevent producing of bending moments.

2.4.1 Adhesion test I

The aluminium substrates are connected with an epoxy adhesive (Renlan M/HY956), considering a 5 mm overlap. The geometrical configuration was selected according to ASTM D1002 [59]. The plates are put under pressure using a 3 kg weight for 24 h and then cured at room temperature for seven days. After curing, five 25.4 mm wide samples (Fig. 5b) are cut from the plate using a band saw; samples cut close to the edge of the plates are discarded due to increased adhesive failure, as recommended by the standard [59]. To obtain the apparent shear strength of the skin to polymer/resin, the tensile tests (Fig. 5c) are performed using a servo-electric Shimadzu AG X-Plus with a crosshead speed of 1.3 mm/min. Three plates are manufactured, and fifteen samples are prepared for lap shear testing. It should be noted that previous studies on the bonding strength of this bonded system have been performed with GFRP specimens in a similar manner to the present study and under the same environmental conditions by the same research group [60]. It is worth mentioning that although the sandwich panels do not have aluminium-aluminium connectivity, the adhesion test I is essential to assess which surface treatment promotes the stronger adhesion to the polymer since this connection generally represents the weakest part of the panel.

2.4.2 Adhesion test II

The adhesion test II is carried out to investigate the bonding strength of the skin/polymer/bamboo adhesive under lap shear loading. Based on notes from ASTM D1002 [59] and ASTM D5868 [61], samples made of aluminium and GFRP substrates were prepared, considering a bamboo ring between the joints. The treated aluminium and GFRP sheets are cut to

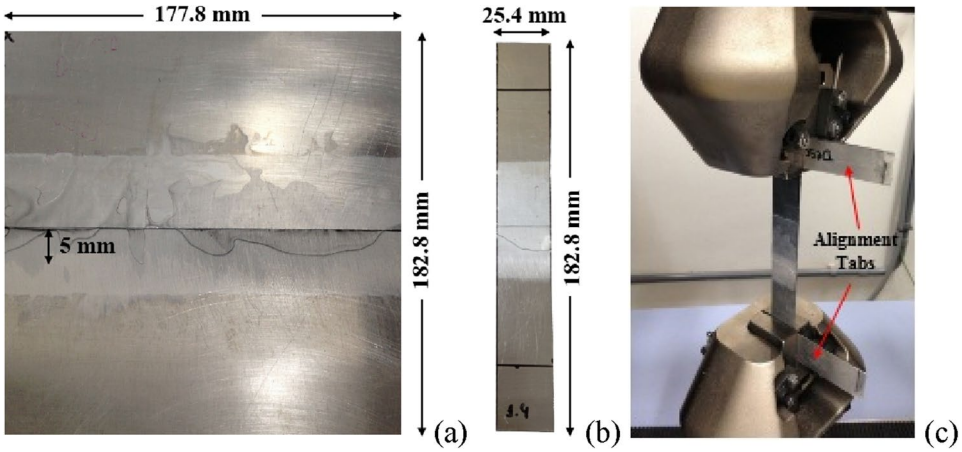

Fig. 5 **a** Aluminium plate with overlapping joint, **b** Specimen for single-lap joint test, **c** Lap shear testing

reach the specimen dimensions presented in Fig. 6a. The epoxy system is prepared manually and spread over the surface of the facesheet, where the bamboo is placed. The thickness of the epoxy layer is 1 mm (Fig. 6b). The Ø25 mm × 3 mm bamboo ring is placed over the adhesive and pressed using a weight of approximately 600 g for 24 h. Then, the face sheet on the opposite side is similarly bonded to the bamboo, resulting in a 25.4 mm wide overlap joint (Fig. 6c). Afterwards, the specimens are cured for seven days at room temperature (Fig. 6d). Finally, the lap shear behaviour of single lap joint samples of skin/polymer/bamboo substrates is evaluated using a Shimadzu AG X-Plus with 1.3 mm/min crosshead speed. It should be pointed out that fifteen samples are tested for each facing material, i.e., aluminium and GFRP.

2.5 Fabrication and testing of sandwich panel specimens

Sandwich panels are fabricated by cold compaction in a wooden mould. Initially, the skin (aluminium or GFRP) is wrapped externally with an adhesive tape to prevent polymer leakage, and subsequently, it is inserted into a mould (Fig. 7a). The epoxy adhesive is then hand-mixed according to the manufacturer's recommendations and poured over the skin, creating a uniform layer of approximately 1 mm thickness. In the next step, the bamboo rings with a height distribution of 13 mm ± 0.05 are inserted one by one according to the diameter and packing geometry of the experimental condition. Figure 7b shows the hexagonal and cubic packing of the bamboo core determined according to the angle and space between adjacent cells. The angle of hexagonal and cubic configurations is equal to 60° and 90°, respectively. The mould is closed with a lid and pressed with a uniform pressure of 2.3 kPa (Fig. 7c) for 24 h at room temperature (~ 22 ℃, 55%RH).

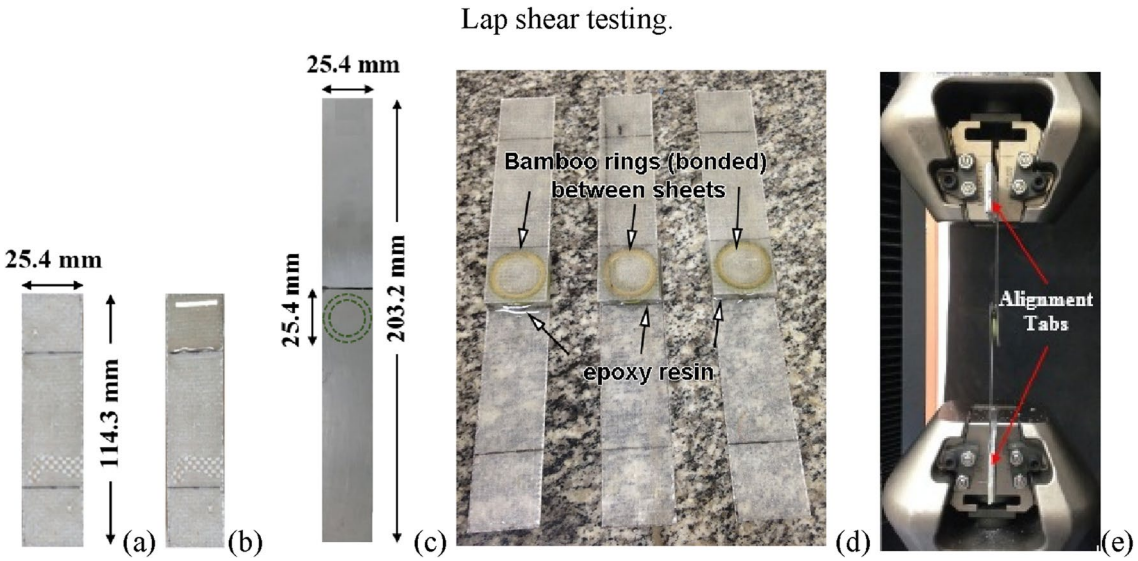

Fig. 6 **a** GFRP sheets for testing, **b** Adhesive application, **c** Specimen dimensions, **d** Cured of specimens and **e** Lap shear testing

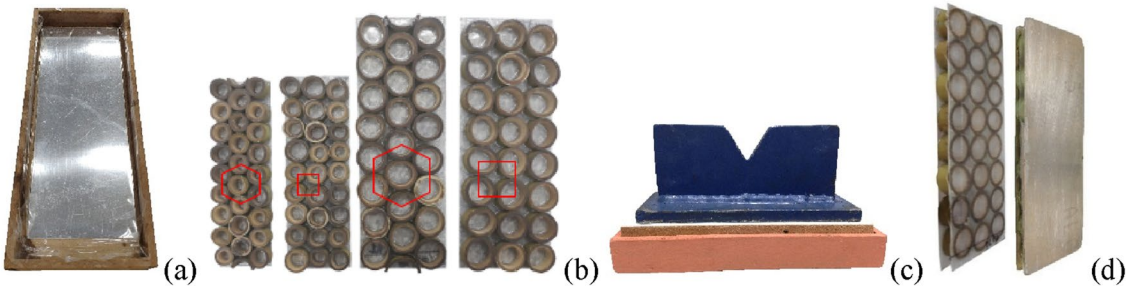

Fig. 7 Sandwich panel manufacturing process: **a** Preparation of aluminium sheets, **b** Bonding of bamboo rings at predefined core configurations (left to right: EC 1 to 4), **c** Application of uniform pressure to join core-face during cure, **d** Final sandwich panel samples.

Afterwards, the material is demoulded, and the opposite face is glued similarly. After 24 h from the mould (Fig. 7d), the sandwich panel is removed and cured for seven days at room temperature (~ 22 ℃, 55%RH). Eight sandwich panels (two replicates of four) are fabricated for each experimental condition for 64 samples.

The sandwich panels are evaluated by a three-point bending test using a 100 kN Shimadzu AG-X Plus (Fig. 8c, d) at 6 mm/min loading speed. Spans of 130 mm and 190 mm are adopted for panels with bamboo rings of Ø20 and Ø30 mm, respectively [62]. The flexural strength (σ_F) and modulus (E_F) are the response/variables evaluated from the bending tests, which consider the entire cross-sectional area as an equivalent homogenous material [50]. The ultimate skin stress (σ_s), ultimate core shear stress (γ_c) and ultimate core shear modulus (G_c) are determined according to Ref. [63, 64]. It is worth mentioning that the equivalent shear properties here assume a high rigidity core [64]. The equivalent density (ρ_{eq}) of the panels is also determined by measuring the weight and dimensions using a precision scale (0.001 g) and a calliper (0.001 mm), respectively.

3 Results and discussion

3.1 Single components

Table 2 shows the properties of the individual components and the adhesion test. The experimental test of aluminium sheets (2024-T3) shows tensile strength and modulus of 350.41 MPa and 74.27 GPa, respectively. The same is also observed for the glass fibre-reinforced polymers [65–67] that possess tensile strength, modulus of elasticity and apparent density of 318.21 MPa, 19.26 GPa and 1.78 g/cm^3, respectively. According to compression and density tests, see Table 2, Ø30 mm bamboo rings have a higher compressive modulus (16%) and a small density (3.33%) than Ø20 mm bamboo rings. A similar trend is also observed by Krause et al. [40]. The compressive properties of bamboo show a quasi-linear correlation with density, implying that a higher density leads to superior mechanical performance.

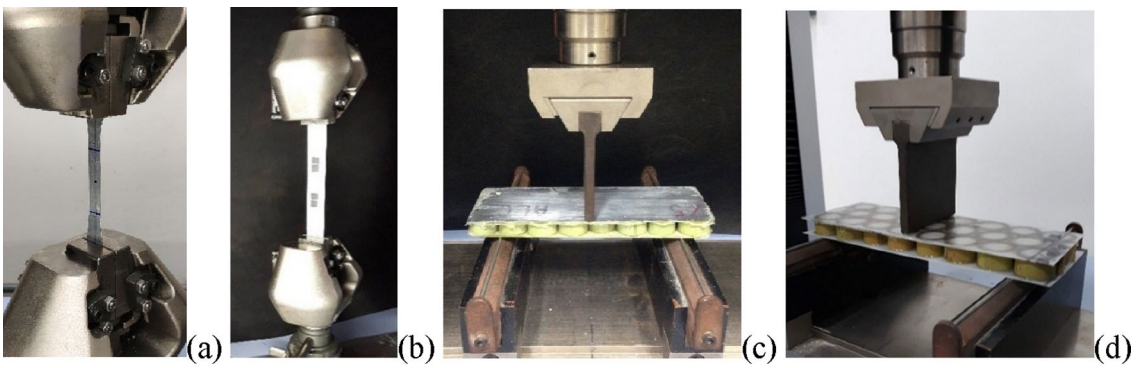

Fig. 8 Tensile test on **a** Aluminium and **b** GFRP; Flexural testing of sandwich panels with **c** Aluminium and **d** GFRP skins

Table 2 Mechanical and physical properties of the aluminium, GFRP, bamboo ring and adhesion test (lap shear)

Component	Tensile		Compressive	Density	Shear strength (Lap shear)
	σ_T (MPa)	E_T (GPa)	E_C (GPa)	ρ (g/cm^3)	$\tau_{s/p}$ [MPa]
Al 2024-T3	350.41 (± 12.83)	74.27 (± 4.61)	–	2.78	8.16 (± 0.26)
GFRP	318.21 (± 15.46)	19.26 (± 1.10)	–	1.78	3.33 (± 0.08)
Bamboo ring Ø20 mm	–	–	11.93	0.90	–
Bamboo ring Ø30 mm	–	–	13.85	0.93	–

3.2 Adhesion test results

The apparent shear strength of the aluminium/polymer joint corresponds to 8.16 MPa, which follows values from open literature [68]. This shear strength is 2.5 times larger than the GFRP/polymer joint, which is 3.33 MPa. According to Wu et al. [56], the difference between shear strengths is due to the presence of micro-roughness on the surface of the aluminium plates after treatment, contrary to the smoother finish of the GFRP. The increased surface roughness of the treated aluminium leads to better mechanical interlocking and consequent bond strength.

On the other hand, the apparent shear strength measured from the adhesion test II cannot be appropriately measured since the shear area is not uniform (see the fractured samples in Fig. 9). However, the shearing behaviour can be assessed from a qualitative standpoint and exhibits an adhesive-type debonding between the face sheet and the polymer, which implies a proper polymer-core adhesion. This fact is attributed to the presence inside the bamboo vessels for water and sap transportation. Those vessels are aligned parallel to the longitudinal axis of the culm and cause an absorption by capillarity, which can lead to increasing the adhesion with the polymer [69]. This absorption mechanism is verified through an absorption test, in which the bamboo rings are weighted and left in a thin layer of polymer for seven days (polymer curing time). Saturation starts right after immersion, as shown in Fig. 10a. After the curing time (Fig. 10b), the excess polymer is removed, and the bamboo is weighted again. This issue results in a polymer absorption of 10.9%, which indicates the excellent state of the bamboo-polymer adhesion.

3.3 Statistical analysis and mechanical test results for the sandwich panels

Table 3 shows the theoretical dimensions of the panels determined following the ASTM C393 standard [62]. The configurations with hexagonal packing are slightly narrower than the cubic ones due to the closer proximity of the rings to the hexagonal configuration. This results in a lower percentage of voids, i.e., non-bamboo filling. Panels with Ø20 mm bamboo have a larger number of rings per volume and, consequently, a lower percentage of voids than Ø30 mm ones. Although the thickness of the aluminium sheets (0.43 mm) is thinner than the one of the GFRPs (0.65 mm), all sandwich panels had a similar total thickness (16.03 ± 0.23 mm) due to the uncertainties linked to the manual production and the non-uniformity of the GFRP compared to the commercial aluminium skins.

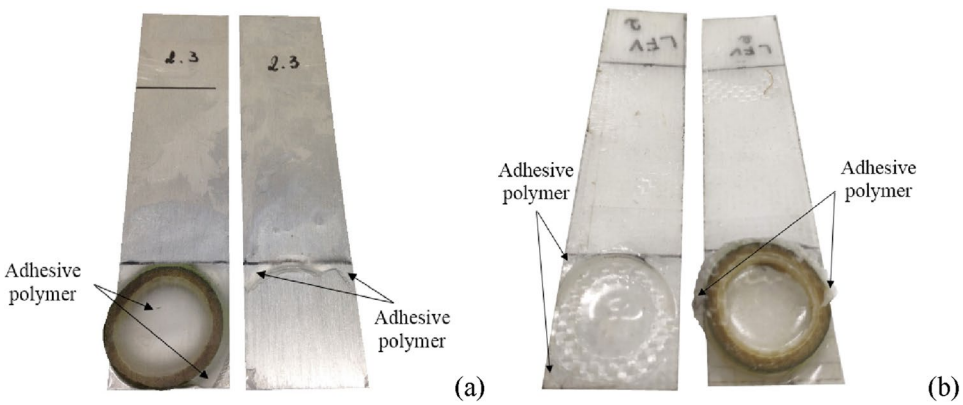

Fig. 9 Fractured specimens of **a** Aluminium and **b** GFRP in the adhesion test II

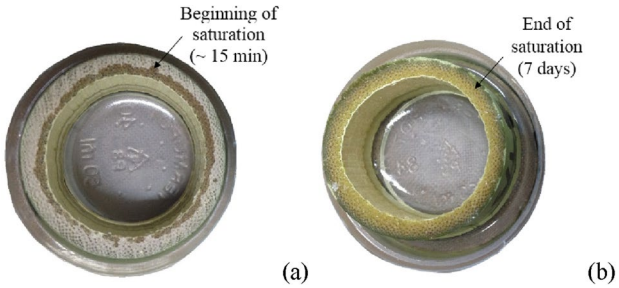

Fig. 10 Absorption test: **a** Beginning and **b** End of saturation

Table 3 Geometrical characteristics of sandwich panels

Sandwich panel	Length (mm)	Width (mm)	Core thickness (mm)	Bamboo rings per panel	Bamboo contact area (mm^2)	Void (%)
Al/GF_20_Hex	180	58	15	27	3711.01	62.51
Al/GF_20_Cub	180	60	15	27	3711.01	65.64
Al/GF_30_Hex	240	88	15	24	5183.63	74.59
Al/GF_30_Cub	240	90	15	24	5183.63	76.00

Table 4 shows the properties of the sandwich panels for replicates 1 and 2. In general, structures made with aluminium skins have superior properties attributed to the enhanced mechanical performance of the single-face sheet material (Table 2) and proper skin-polymer adhesion. The effect of the face skin material, bamboo diameter and packing geometry on the physical and mechanical properties of the sandwich panels are interpreted statistically in the following section.

3.3.1 Statistical analysis

Table 5 shows the analysis of variance (ANOVA) of the DoE responses. Values in bold represent statistically significant effects with a 95% confidence level (P-value ≤ 0.05), while underlines indicate higher-order effects and will be interpreted using effect plots. The main effect of a factor should be analysed individually only if there is no other evidence of significant interactions amongst factors, as is the case for the Facing Material of the Equivalent Density. The R^2-adjusted varies from 93.45% to 99.77%, indicating models of high predictability. The Anderson–Darling normality test validates the ANOVA since the P-values are above 0.05 (0.239–0.996), implying that the data follow a normal distribution.

Figure 11 shows the main and second-order interaction effects for the mean (average) equivalent density. Sandwich panels with GFRP skins exhibit a 4% reduction in response (Fig. 11a); this is attributed to the low density of this composite compared to the case with aluminium sheets (Table 2). The interaction between the packing geometry and the bamboo diameter (Fig. 11b) shows that the sandwich panels with cubic configuration and Ø30 mm bamboo rings have the lowest density (reduction of 17%), which is attributed to the larger percentage of voids (see Table 3) and less structural weight. Although Ø20 mm bamboo rings have a slightly lower density, an increase in this response is observed for these panels, especially when considering the hexagonal packing. This is due to the larger mass and closer proximity (i.e., lower volume) of these rings.

Figure 12 shows the third-order interaction effects for the mean flexural strength. The use of aluminium skins, Ø30 mm bamboo rings and hexagonal packing in sandwich panels results in configurations with the largest flexural strength. The greater apparent shear strength of the aluminium/polymer bond plays an essential role in increasing the flexural strength of the panel since this response is mainly related to the core-face bonding [45]. In addition, aluminium sheets have a 10% higher tensile strength than the GFRP ones, contributing to the withstanding of a higher flexural load. The Ø30 mm bamboo rings increase the flexural strength because they are present in small amounts in the sandwich panels (see Table 3), resulting in less variation in the adhesive thickness and a better bonding quality than the configurations with Ø20 mm. Hexagonal packing of the core also improves flexural strength due to the greater number of constraints. This fact is also reported by Hu et al. [70]. They observed that the six neighbouring rings of the hexagonal configuration result in denser packaging than the four adjacent cubic configurations. The improved packaging provides a core with an enhanced capacity to withstand the flexural load.

Table 4 Mechanical of the sandwich panels

	E.C	Equivalent density (g/cm^3)	Flexural strength (MPa)	Flexural modulus (GPa)	Ultimate skin stress (MPa)	Ultimate core shear stress (MPa)	Ultimate core shear modulus (MPa)
Replicate 1	Al_20_Hex	0.590 (±0.033)	30.10 (±1.99)	6.36 (±0.30)	190.46 (±10.15)	3.33 (±0.34)	132.00 (±10.59)
	Al_20_Cub	0.544 (±0.021)	26.53 (±2.90)	5.94 (±0.45)	167.72 (±13.76)	2.94 (±0.23)	125.56 (±11.79)
	Al_30_Hex	0.513 (±0.009)	43.21 (±2.11)	7.61 (±0.22)	288.00 (±32.76)	3.33 (±0.23)	78.59 (±2.63)
	Al_30_Cub	0.498 (±0.005)	32.43 (±1.10)	6.87 (±0.42)	204.28 (±21.21)	2.42 (±0.32)	69.42 (±4.83)
	GF_20_Hex	0.569 (±0.033)	28.65 (±1.49)	3.35 (±0.58)	130.64 (±9.33)	3.31 (±0.45)	71.11 (±2.63)
	GF_20_Cub	0.519 (±0.025)	25.45 (±3.42)	3.24 (±0.28)	105.76 (±9.35)	2.63 (±0.35)	64.76 (±5.24)
	GF_30_Hex	0.489 (±0.017)	34.65 (±2.80)	4.10 (±0.48)	142.77 (±4.46)	2.91 (±0.18)	40.07 (±3.76)
	GF_30_Cub	0.475 (±0.001)	29.85 (±0.61)	3.90 (±0.21)	127.69 (±3.52)	2.40 (±0.16)	36.94 (±3.48)
Replicate 2	Al_20_Hex	0.596 (±0.004)	30.99 (±1.92)	6.29 (±0.36)	194.63 (±13.58)	3.58 (±0.22)	131.75 (±11.92)
	Al_20_Cub	0.565 (±0.010)	27.30 (±1.42)	6.12 (±0.49)	172.64 (±15.23)	2.97 (±0.37)	121.51 (±15.69)
	Al_30_Hex	0.514 (±0.008)	43.38 (±2.41)	7.52 (±0.39)	280.64 (±23.03)	3.25 (±0.17)	80.90 (±3.90)
	Al_30_Cub	0.486 (±0.005)	31.70 (±0.84)	6.95 (±0.03)	208.78 (±16.79)	2.49 (±0.24)	73.10 (±2.34)
	GF_20_Hex	0.572 (±0.020)	28.08 (±1.07)	3.38 (±0.44)	123.41 (±8.43)	3.15 (±0.42)	68.65 (±4.45)
	GF_20_Cub	0.539 (±0.027)	24.78 (±2.54)	3.02 (±0.35)	101.54 (±7.47)	2.75 (±0.32)	62.69 (±4.17)
	GF_30_Hex	0.490 (±0.003)	33.35 (±1.14)	4.10 (±0.28)	142.27 (±6.32)	2.70 (±0.24)	38.90 (±3.63)
	GF_30_Cub	0.477 (±0.005)	28.35 (±0.78)	3.84 (±0.01)	125.76 (±4.43)	2.41 (±0.01)	37.58 (±2.92)

Table 5 Analysis of variance for the mechanical properties of sandwich panels

Factors and interactions	P-value					
	Equivalent density	Flexural strength	Flexural modulus	Skin stress	Core shear stress	Core shear modulus
Facing material (FM)	**0.001**	**0.000**	**0.000**	**0.000**	**0.001**	**0.000**
Bamboo diameter (BD)	**0.000**	**0.000**	**0.000**	**0.000**	**0.000**	**0.000**
Packing geometry (PG)	**0.000**	**0.000**	**0.000**	**0.000**	**0.000**	**0.000**
FM * BD	0.633	**0.000**	**0.004**	**0.000**	0.797	**0.000**
FM * PG	0.783	**0.001**	**0.016**	**0.000**	0.078	**0.040**
BD * PG	**0.022**	**0.000**	0.055	**0.000**	0.379	0.302
FM * BD * PG	0.520	**0.002**	0.059	**0.000**	**0.047**	0.270
R^2—adj	96.22%	98.61%	99.77%	99.63%	93.45%	99.74%
Anderson–Darling (P-value ≥ 0.05)	0.252	0.298	0.935	0.239	0.996	0.899

Table 5 shows the analysis of variance (ANOVA) of the DoE responses. Values in bold represent statistically significant effects witha 95% confidence level (P-value ≤ 0.05), while underlines indicate higher-order effects and will be interpreted using effect plots.

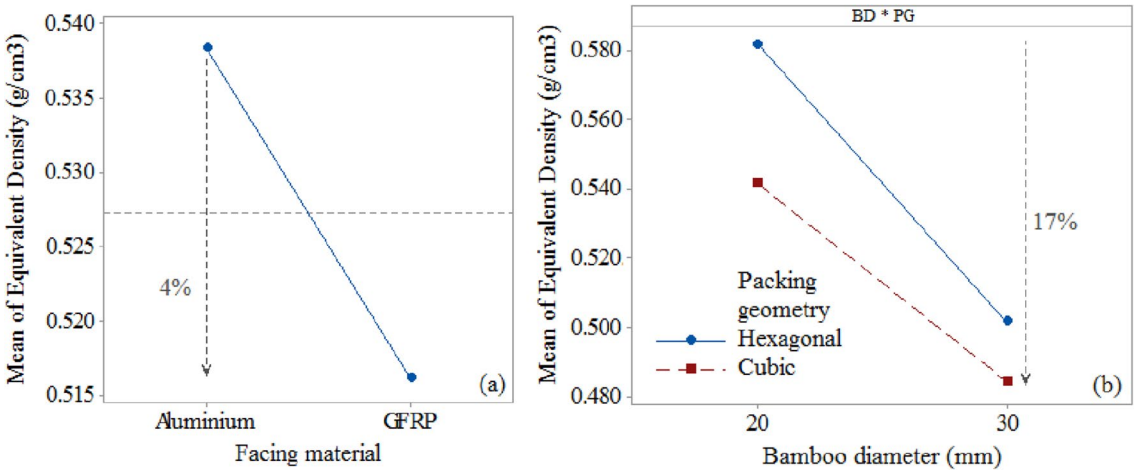

Fig. 11 Effect plot for the mean (average) equivalent density

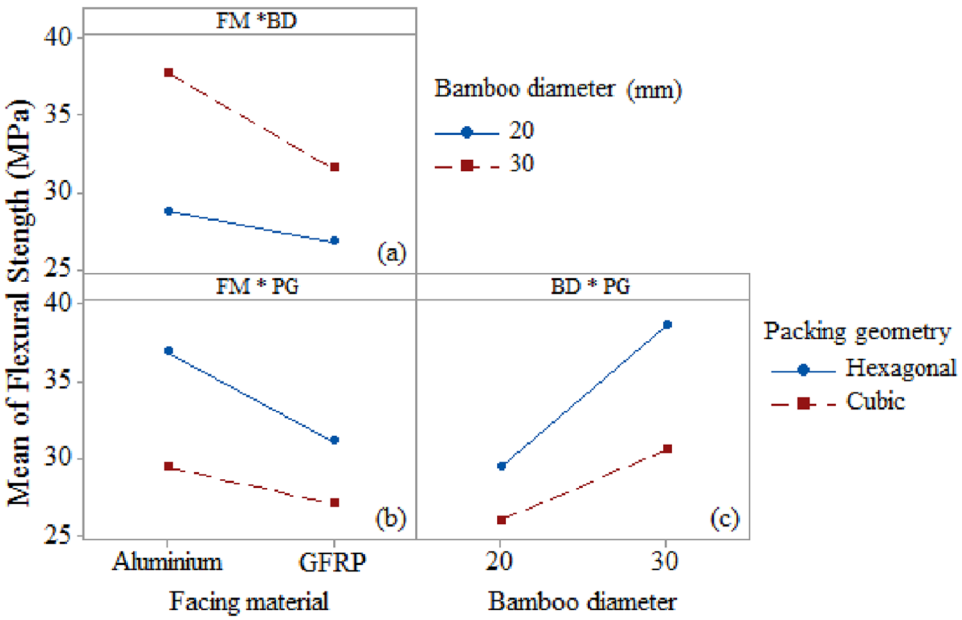

Fig. 12 Third-order interaction effect for the mean (average) flexural strength

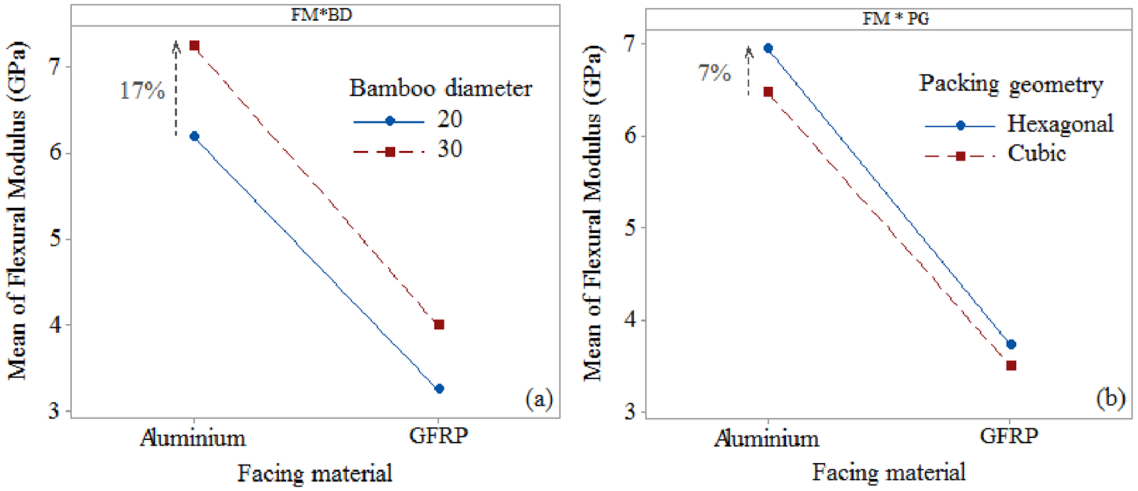

Fig. 13 Second-order interaction effect plots for the mean flexural modulus

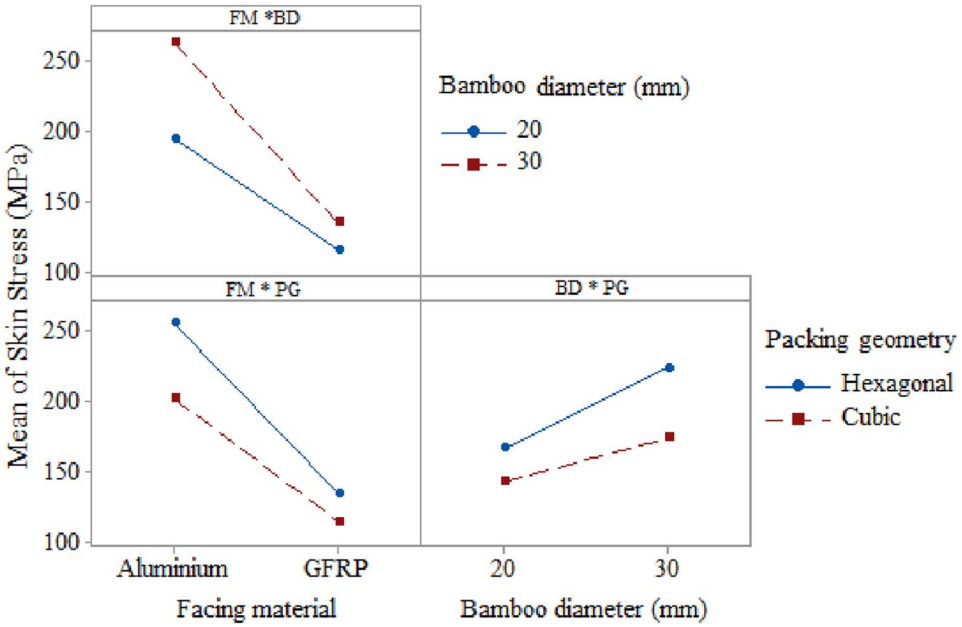

Fig. 14 Third-order interaction effect plot for the mean skin stress

Figure 13 shows the second-order interaction effects for the mean flexural modulus. The interaction between aluminium skins with Ø30 mm bamboo rings (Fig. 13a) and the hexagonal geometry (Fig. 13b) results in the largest flexural modulus, exhibiting behaviour similar to the one related to flexural strength. The aluminium sheets have a tensile modulus of more than three times greater than the GFRP ones (Table 2), which contributes to the increasing rigidity of the panel under flexural load. The use of Ø30 mm bamboo rings increases up to 17% (Fig. 13a) in terms of stiffness and less deflection during the elastic deformation; this is due to the larger compressive modulus and good bonding quality of those rings. The closer proximity of the core present in the hexagonal packing leads to a more significant number of constraints, decreasing the mobility of the rings and increasing the rigidity by up to 7% under flexural load (Fig. 13b).

Figure 14 shows the third-order interaction effect plots for the mean skin stress. The trend is similar to the results pertaining the flexural strength, since the skin stress is determined considering that the faces support the entire flexural load via compressive and tensile efforts [62]. Sandwich panels made with aluminium skins and Ø30 mm bamboo rings, and hexagonal packing achieve the highest skin stress. This behaviour can be attributed to the greater mechanical properties of the aluminium sheets, the proper bonding quality of the Ø30 mm bamboo rings and a larger number of constraints present in the hexagonal packing. The synergistic effect of these parameters contributes to increasing the skin stress of the sandwich panels. Although this response is related to the ability of the face skins to withstand the tensile and

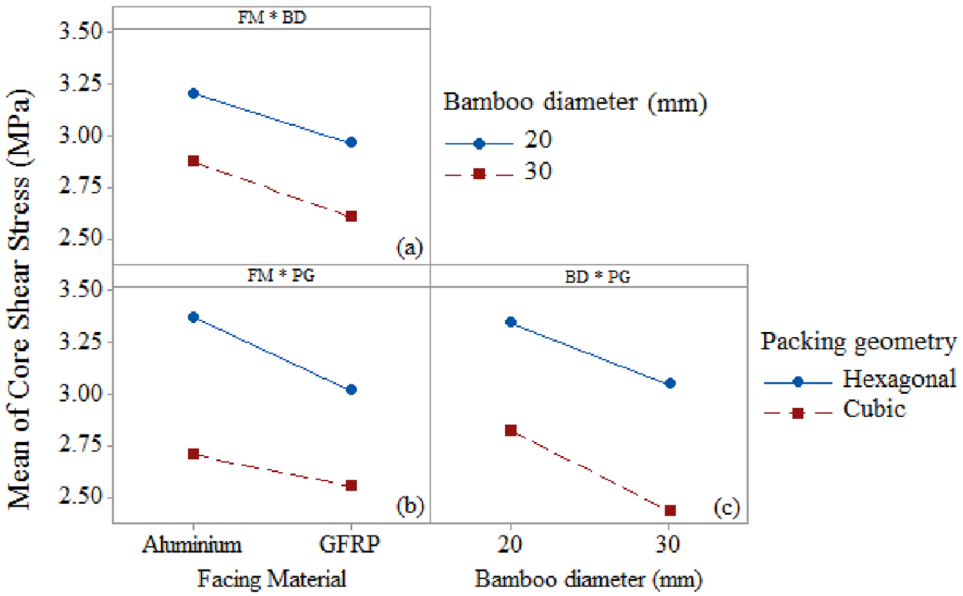

Fig. 15 Third-order interaction effect plot for the mean core shear stress

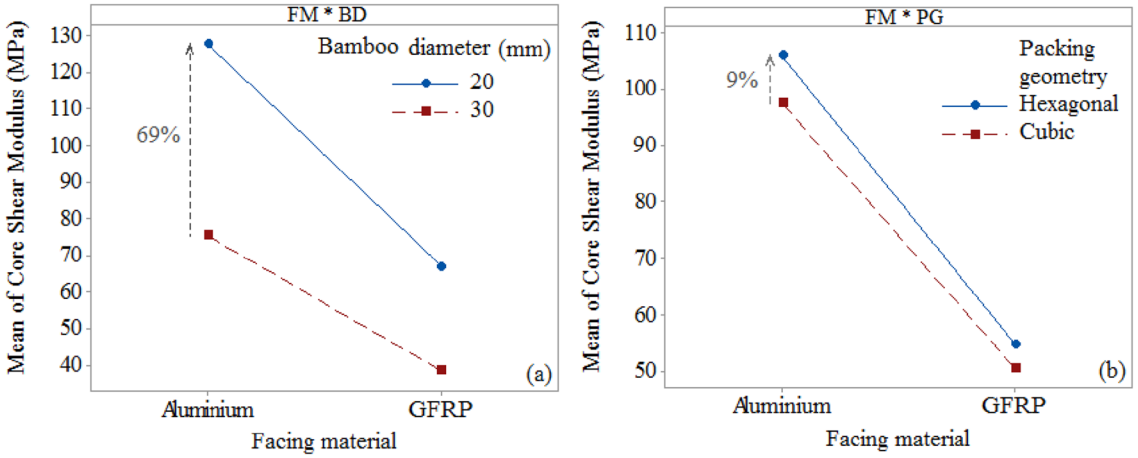

Fig. 16 Second-order interaction effect plots for the mean core shear modulus

compressive loads, the results highlight the importance of the characteristics of the core within the structural performance of a sandwich panel, since both factors (cell diameter and packing geometry) significantly affect this response.

Figure 15 shows the third-order interaction effects for the mean core shear stress. The use of the aluminium skins and the hexagonal packing geometry (Fig. 15b) increases the core shear stress, which is in accordance with the other responses. Again, this is attributed to the superior mechanical performance of the aluminium sheets and the closeness of the rings in this configuration, supporting larger shear stresses. The high degree of aluminium/polymer bonding positively contributes to the core shear properties. In this case, the panels support the largest flexural load, transferring it to the core before failure. However, an opposite behaviour to the other responses is observed for the bamboo diameter factor, exhibiting an increase in the core shear stress when Ø20 mm bamboo rings are used (Fig. 15a and c). The same behaviour is observed by Oliveira et al. [45]: smaller diameters of bamboo rings provide larger shear stresses due to the greater number of bamboo rings per volume and a lower percentage of voids, thus increasing the shear constraints.

Figure 16 shows the second-order interaction effects for the mean (average) core shear modulus. The interaction between aluminium skins with Ø20 mm bamboo rings (Fig. 16a) and hexagonal geometry (Fig. 16b) results in the largest core shear modulus, with a behaviour similar to the one related to the core shear stress. The use of Ø20 mm bamboo rings, which results in increases of up to 69% (Fig. 16a), requires greater efforts during shear deformation due to their larger number per volume and a lower percentage of voids. The closer proximity of the core for the hexagonal packing

leads to a greater number of constraints, decreasing the mobility of the rings and increasing the rigidity by up to 9% under shear load (Fig. 16b).

3.4 Failure analysis

Figure 17 shows representative load-displacement curves for sandwich panels made of aluminium and GFRP skins under flexural load. The flexural load ranges from 1985 N (GF_20_Cub) to 3562 N (Al_30_Hex). The sandwich panels with aluminium and GFRP skins have a similar trend, achieving the maximum load and displacement for Ø30 mm bamboo rings and hexagonal packing, following the flexural strength response.

Sandwich panels with aluminium skins (Fig. 17a) exhibit a significant elastic deformation, followed by a sudden drop with a catastrophic failure. This failure mode is attributed to a detachment between the bottom skin and the adhesive layer, as shown in Fig. 18, which follows the adhesion test results ("Adhesion test results" Section). Due to its several internal vessels, bamboo has a stronger bonding with the polymer than with aluminium. Thus, improving this type of adhesion may constitute the scope of future investigations to increase the structural performance of the panel. The aluminium skins do not present any damage since the skin stress (see Table 4) is below the ultimate tensile strength of the aluminium sheets (350.41 MPa, see Table 2).

On the other hand, sandwich panels made with GFRP skins (Fig. 17b) have a smoother and extended elastic behaviour, followed by a slight plastic deformation before the failure drop. This failure mode is attributed to breaking the upper skin (Fig. 19) that is in contact with the actuator. Although the skin stress of the GFRPs (see Table 4) does not exceed the ultimate tensile strength of the composite (318.21 MPa, see Table 2), the upper face is less resistant under compressive efforts [65], resulting in the cracked matrix (dashed in red). The matrix phase governs the compressive behaviour of FRPs. The compressive strength of the epoxy system (69.55 MPa) is lower than the stresses achieved by the skins (Fig. 14). The sandwich panel does not show core-face debonding despite its low skin/polymer adhesion; this indicates a premature failure with loss of structural performance right after face cracking.

3.5 Comparison to commercially available structures

Table 6 compares the proposed sandwich panel's absolute and specific properties with the core having the highest mechanical performance under quasi-static load (the Al_30_Hex) and two commercial panels used in the aeronautical industry: the Gillfloor® 5425 and Gillfab® 4030. Gillfloor® 5425 consists of a honeycomb structure made of unidirectional glass fibre composite skins and a 5052 aluminium honeycomb core, commonly used in walk-in areas on aircraft, such as aisles and entries of the Boeing 737–800 [71]. The Gillfab® 4030 consists of a structural panel composed of 2024-T3 aluminium skins and a 5052 aluminium honeycomb core, commonly used in internal aircraft applications, including bulkheads, shelving and galley panels [72]. Both structures use epoxy polymer as the adhesive. An approximate equivalent density of commercial sandwich panels is determined by considering the thickness of the panels, from which the specific properties (ratio between absolute properties and equivalent density) can be estimated.

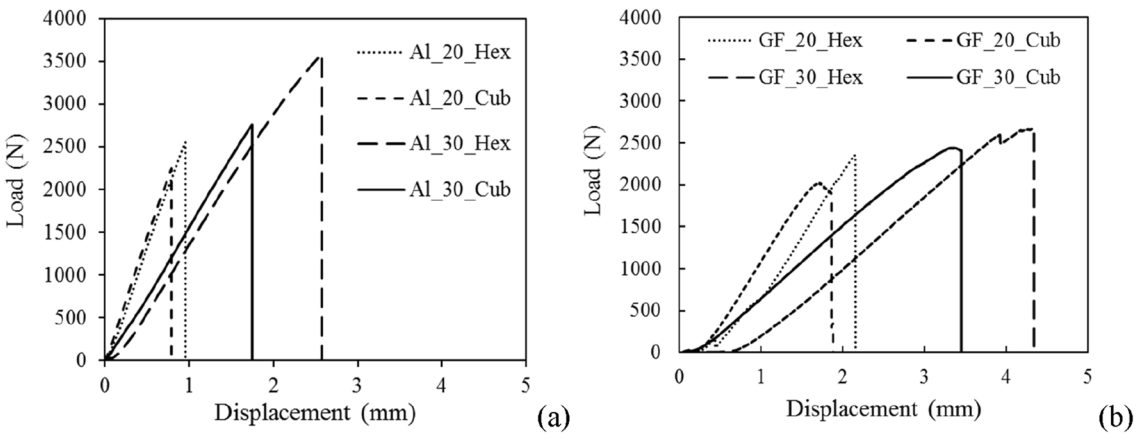

Fig. 17 Load-displacement curves for sandwich panels made with **a** Aluminium and **b** GFRP skins

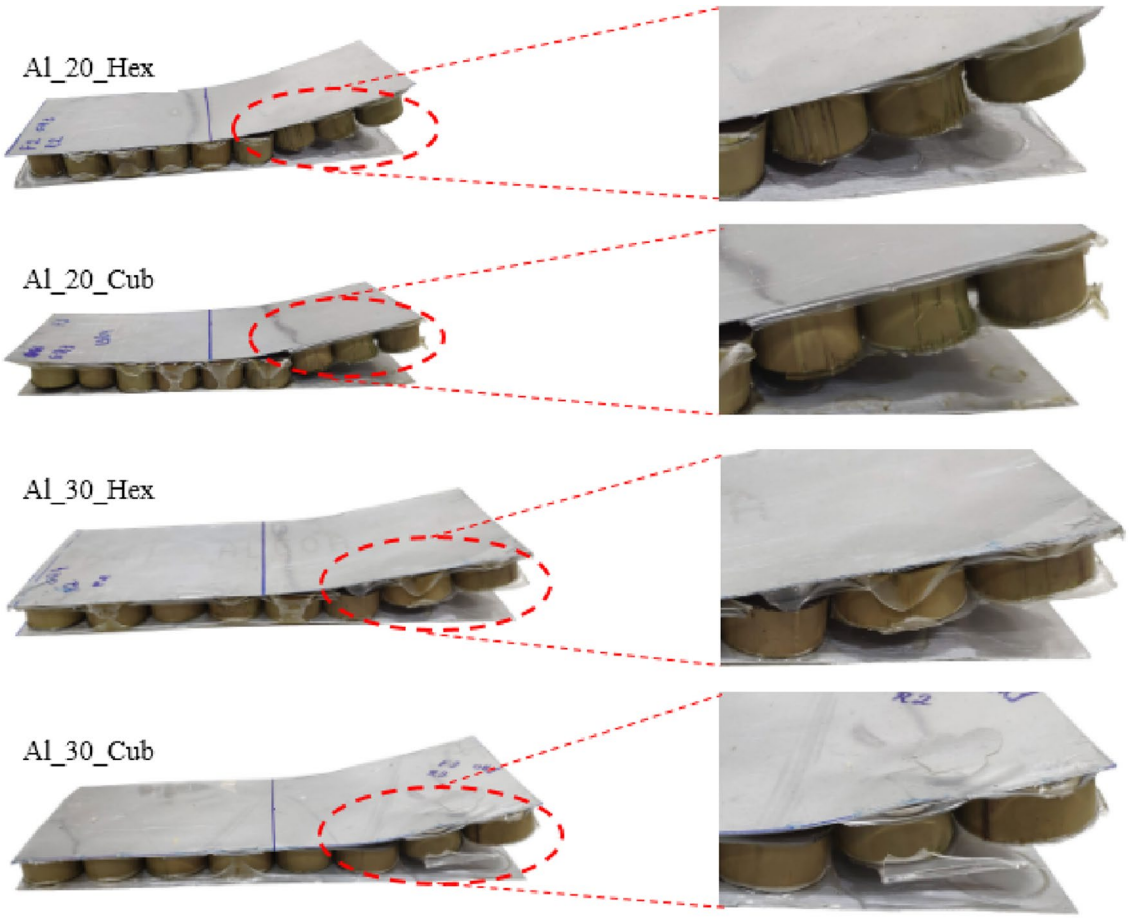

Fig. 18 Failure modes of the sandwich panels with aluminium skins

According to Table 6, the absolute properties of the Al_30_Hex panels are comparable to those of the commercial sandwich structures, while the specific properties are slightly lower. More studies involving other parameters are still required to assess a practical application, including thermal, acoustic and—most importantly—flammability testing and full-scale mechanical analysis. Nevertheless, the Al_30_Hex developed here shows to be a potentially feasible and sustainable alternative for future secondary-structural frames in transport used for flooring, interior components, cargo bays, containers, and split walls.

4 Conclusions

The mechanical behaviour of sandwich panels made with a bamboo core of different dimensions, packing geometries and facing materials have been investigated using statistical analyses. Physical–mechanical characterisation and interfacial bonding tests have also assessed the individual components. The main conclusions of this work are the following:

i. Treated aluminium sheets type 2024-T3 have larger tensile properties and adhesive strength than GFRP skins. Aluminium sheets contribute to the increase of the flexural and shear properties of the sandwich panel made with this type of skin;

ii. The high absorption of the polymer by the bamboo ring increases the bonding at the interface, resulting in a debonding occurring between skin and polymer;

iii. The equivalent density of the sandwich panels is affected by the type of material of the face skins and the percentage of voids, resulting in a decrease of the same density when GFRP are adopted together with larger bamboo rings (Ø30 mm) and the use of a cubic packing;

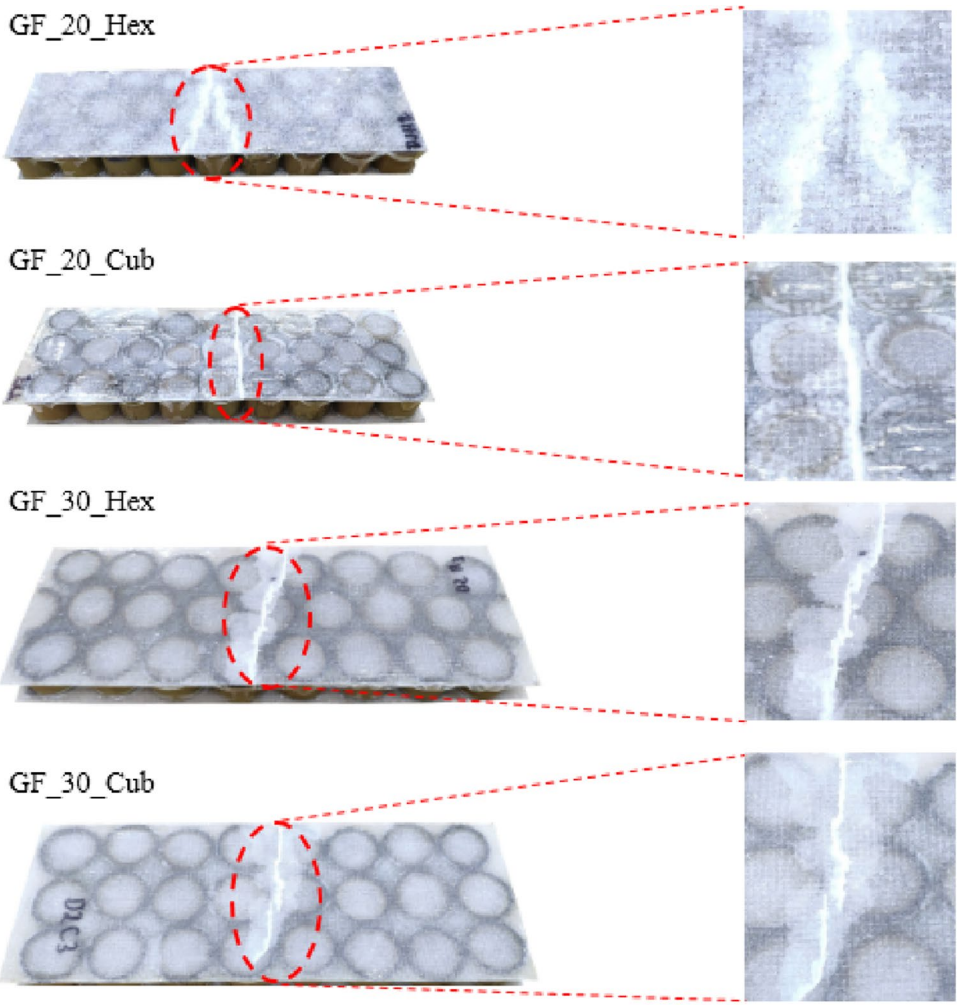

Fig. 19 Failure modes of the sandwich panels with GFRP skins

Table 6 Comparison between the proposed sandwich panel and commercial structures

Property	Al_30_Hex	Gillfloor® 5424 [64]	Gillfab® 4030 [65]
Equivalent density (g/cm^3)	0.513	0.303	0.346
Flexural modulus (GPa)	7.57	3.10	–
Specific flexural modulus (kN.m.g^{-1})	14.76	10.23	–
Skin stress (MPa)	284.32	202.52	290
Specific skin stress (N.m.g^{-1})	554.23	668.38	838.15
Core shear stress (MPa)	3.29	–	3.39
Specific core shear stress (N.m.g^{-1})	6.41	–	9.80

iv. Sandwich panels with aluminium skins, Ø30 mm bamboo rings, and hexagonal packing provide enhanced flexural properties and skin stresses, while those with Ø20 mm bamboo rings show the most considerable shear stiffness and strength performance;

v. Sandwich panels with aluminium skins exhibit debonding between the bottom skin and the adhesive, while those with GFRP sheets present a premature failure with face crack and loss of structural performance;

vi. The proposed sandwich panels have a mechanical performance comparable to existing commercial structures, representing a potentially sustainable alternative to replace secondary structural components in future transport facilities.

Acknowledgements The authors would like to thank the Brazilian Research Agencies, CAPES (PhD scholarship), CNPq (PQ 309885/2019-1, PDJ 163562/2020-2) and FAPEMIG (PPM and undergraduate grant), for the financial support and the Faculty of Engineering and the Bristol Composites Institute and UFSJ for the infrastructure provided.

Author contributions LO: Investigation, data curation, writing—original draft preparation. MV: Investigation, data curation. RF: Supervision, data curation, writing- reviewing and editing. JS: Investigation, methodology, writing—original draft preparation. MLPT: Methodology, writing—reviewing and editing. THP: Supervision, resources, conceptualization, methodology, writing—reviewing and editing. PZ: Data curation, writing—reviewing and editing. FS: Supervision, resources, writing- reviewing and editing. All authors read and approved the final mansucritpt.

Funding Tulio Hallak Panzera: CNPq-Brazil (PQ 309885/2019-1) & FAPEMIG (PPM-00075-17). Livia Oliveira: CAPES-Brazil (PhD scholarship). Matheus Vieira: FAPEMIG (undergraduate Grant). Julio César dos Santos (Post doc Grant, CNPq 163,562/2020-2).

Data availability The raw/processed data required to reproduce these findings cannot be shared at this time as the data also forms part of an ongoing study.

Declarations

Competing interests The authors declare that they have no competing interests.

References

1. Tan HL, He ZC, Li E, Tan XW, Cheng AG, Li QQ. Energy absorption characteristics of three-layered sandwich panels with graded re-entrant hierarchical honeycombs cores. Aerosp Sci Technol. 2020. https://doi.org/10.1016/j.ast.2020.106073.
2. Naik RK, Panda SK, Racherla V. A new method for joining metal and polymer sheets in sandwich panels for highly improved interface strength. Compos Struct. 2020;251:112661. https://doi.org/10.1016/j.compstruct.2020.112661.
3. Noor AK, Burton WS, Bert CW. Computational models for sandwich panels and shells. Appl Mech Rev. 1996. https://doi.org/10.1115/13101923.
4. Liu K, Zong S, Li Y, Wang Z, Hu Z, Wang Z. Structural response of the U-type corrugated core sandwich panel used in ship structures under the lateral quasi-static compression load. Mar Struct. 2022;84:103198. https://doi.org/10.1016/j.marstruc.2022.103198.
5. Wang J, Shi C, Yang N, Sun H, Liu Y, Song B. Strength, stiffness, and panel peeling strength of carbon fibre-reinforced composite sandwich structures with aluminum honeycomb cores for vehicle body. Compos Struct. 2018;184:1189–96. https://doi.org/10.1016/j.compstruct.2017.10.038.
6. Önder A, Robinson M. Investigating the feasibility of a new testing method for GFRP/polymer foam sandwich composites used in railway passenger vehicles. Compos Struct. 2020;233:111576. https://doi.org/10.1016/j.compstruct.2019.111576.
7. Soleymani M, Tahani M, Zamani P. On the influence of resin pocket area on the failure of tapered sandwich composites. Adv Struct Eng. 2021;24(1):42–51.
8. Oliveira PR, Panzera TH, Freire RT, Scarpa F. Sustainable sandwich structures made from bottle caps core and aluminium skins: a statistical approach. Thin Wall Struct. 2018;130:362–71. https://doi.org/10.1016/j.tws.2018.06.003.
9. Cai S, Liu J, Zhang P, Li C, Cheng Y. Dynamic response of sandwich panels with multi-layered aluminum foam/UHMWPE laminate cores under air blast loading. Int J Impact Eng. 2020;138:103475. https://doi.org/10.1016/j.ijimpeng.2019.103475.
10. Usta F, Türkmen HS, Scarpa F. High-velocity impact resistance of doubly curved sandwich panels with re-entrant honeycomb and foam core. Int J Impact Eng. 2022;165:104230. https://doi.org/10.1016/j.ijimpeng.2022.104230.
11. Zhao D, Liu T, Lu X, Meng X. Experimental and numerical analysis of a novel curved sandwich panel with pultruded GFRP strip core. Compos Struct. 2022;288:115404. https://doi.org/10.1016/j.compstruct.2022.115404.
12. Salgado IP, Silva FA. Flexural behavior of sandwich panels combining curauá fiber-reinforced composite layers and autoclaved aerated concrete core. Constr Build Mater. 2021. https://doi.org/10.1016/j.conbuildmat.2021.122890.
13. Cui Y, Hao H, Li J, Chen W, Zhang X. Structural behavior and vibration characteristics of geopolymer composite lightweight sandwich panels for prefabricated buildings. J Build Eng. 2022. https://doi.org/10.1016/j.jobe.2022.104872.
14. Kavermann SW, Bhattacharyya D. Experimental investigation of the static behaviour of a corrugated plywood sandwich core. Compos Struct. 2019;207:836–44. https://doi.org/10.1016/j.compstruct.2018.09.094.
15. Oliveira PR, May M, Panzera TH, Scarpa F, Hiermaier S. Improved sustainable sandwich panels based on bottle caps core. Compos Part B. 2020;199:108165. https://doi.org/10.1016/j.compositesb.2020.108165.
16. Feng Y, Qiu H, Gao Y, Zheng H, Tan J. Creative design for sandwich structures: a review. Int J Adv Robot Syst. 2020. https://doi.org/10.1177/1729881420921327.

17. Ma M, Yao W, Jiang W, Jin W, Chen Y, Li P. Fatigue behavior of composite sandwich panels under three point bending load. Polym Test. 2020. https://doi.org/10.1016/j.polymertesting.2020.106795.
18. Pareta AS, Gupta R, Panda SK. Experimental investigation on fly ash particulate reinforcement for property enhancement of PU foam core FRP sandwich composite. Compos Sci Technol. 2020. https://doi.org/10.1016/j.compscitech.2020.108207.
19. Yuan H, Zhang J, Sun H. The failure behavior of double-layer metal foam sandwich beams under three-point bending. Thin Wall Struct. 2022. https://doi.org/10.1016/j.tws.2022.109801.
20. Mohammadabadi M, Yadama V, Smith L. The effect of plate theories and boundary conditions on the bending behavior of a biaxial corrugated core sandwich panel. Compos Struct. 2020. https://doi.org/10.1016/j.compstruct.2020.112133.
21. Xia F, Durandet Y, Tan PJ, Ruan D. Three-point bending performance of sandwich panels with various types of cores. Thin Wall Struct. 2022. https://doi.org/10.1016/j.tws.2022.109723.
22. Norouzi H, Rostamiyan Y. Experimental and numerical study of flatwise compression behavior of carbon fibre composite sandwich panels with new lattice cores. Constr Build Mater. 2015;100:22–30. https://doi.org/10.1016/j.conbuildmat.2015.09.046.
23. Cai Z-Y, Zhang X, Liang X-B. Multi-point forming of sandwich panels with egg-box-like cores and failure behaviors in forming process: analytical models, numerical and experimental investigations. Mater Des. 2018;160:1029–41. https://doi.org/10.1016/j.matdes.2018.10.037.
24. Madke RR, Chowdhury R. Anti-impact behavior of auxetic sandwich structure with braided face sheets and 3D re-entrant cores. Compos Struct. 2020. https://doi.org/10.1016/j.compstruct.2019.111838.
25. Zhu K, Zheng X, Zhang C, Chen N, Han Y, Yan L, Quaresimin M. Compressive response and energy absorption of all-composite sandwich panels with channel cores. Compos Struct. 2022. https://doi.org/10.1016/j.compstruct.2022.115461.
26. Anbusagar NRR, Palanikumar K, Giridharan PK. Study of sandwich effect on nanoclay modified polyester resin GFR face sheet laminates. Compos Struct. 2015;125:336–42. https://doi.org/10.1016/j.compstruct.2015.02.016.
27. Gholami M, Alashti RA, Fathi A. Optimal design of a honeycomb core composite sandwich panel using evolutionary optimisation algorithms. Compos Struct. 2016;139:254–62. https://doi.org/10.1016/j.compstruct.2015.12.019.
28. Benzidane MA, Benzidane R, Hamamousse K, Adjal Y, Sereir Z, Poilâne C. Valorization of date palm wastes as sandwich panels using short rachis fibers in skin and petiole 'wood' as core. Ind Crop Prod. 2022;177:114436. https://doi.org/10.1016/j.indcrop.2021.114436.
29. Oliveira PR, May M, Panzera TH, Hiermaier S. Bio-based/green sandwich structures: a review. Thin Wall Struct. 2022;177:109426. https://doi.org/10.1016/j.tws.2022.109426.
30. Dutra JR, Filho SLMR, Christoforo AL, Panzera TH, Scarpa F. Investigations on sustainable honeycomb sandwich panels containing eucalyptus sawdust, Piassava and cement particles. Thin Wall Struct. 2019;143:106191. https://doi.org/10.1016/j.tws.2019.106191.
31. Oliveira PR, May M, Panzera TH, Scarpa F, Hiermaier S. Reinforced biobased adhesive for eco-friendly sandwich panels. Int J Adhes Adhes. 2020;98:102550. https://doi.org/10.1016/j.ijadhadh.2020.102550.
32. Kopparthy SDS, Netravali AN. Review: green composites for structural applications. Composites Part C: Open Access. 2021;6:100169. https://doi.org/10.1016/j.jcomc.2021.100169.
33. Pozzer T, Gauss C, Barbirato GHA, Fiorelli J. Trapezoidal core sandwich panel produced with sugarcane bagasse. Constr Build Mater. 2020;264:120718. https://doi.org/10.1016/j.conbuildmat.2020.120718.
34. Xu P, Zhu J, Li H, Wei Y, Xiong Z, Xu X. Are bamboo construction materials environmentally friendly? A life cycle environmental impact analysis. Environ Impact Asses. 2022;96:106853. https://doi.org/10.1016/j.eiar.2022.106853.
35. Li H-T, Su J-W, Zhang Q-S, Deeks AJ, Hui D. Mechanical performance of laminated bamboo column under axial compression. Compos Part B. 2015;79:374–82. https://doi.org/10.1016/j.compositesb.2015.04.027.
36. Abdul Khalil HPS, Bhat IUH, Jawaid M, Zaidon A, Hermawan D, Hadi YS. Bamboo fibre reinforced biocomposites: a review. Mater Des. 2012. https://doi.org/10.1016/j.matdes.2012.06.015.
37. Jakovljevic S, Lisjak D, Alar Z, Penava F. The influence of humidity on mechanical properties of bamboo for bicycles. Constr Build Mater. 2017;150:35–48. https://doi.org/10.1016/j.conbuildmat.2017.05.189.
38. Li W-T, Long Y-L, Huang J, Lin Y. Axial load behavior of structural bamboo filled with concrete and cement mortar. Constr Build Mater. 2017;148:273–87. https://doi.org/10.1016/j.conbuildmat.2017.05.061.
39. Bhagat D, Bhalla S, West RP. Fabrication and structural evaluation of fibre reinforced bamboo composite beams as green structural elements. Compos Part C. 2021;5:100150. https://doi.org/10.1016/j.jcomc.2021.100150.
40. Krause JQ, Silva FA, Ghavami K, Gomes OFM, Filho RDT. On the influence of *Dendrocalamus giganteus* bamboo microstructure on its mechanical behavior. Constr Build Mater. 2016;127:199–209. https://doi.org/10.1016/j.conbuildmat.2016.09.104.
41. Darzi S, Karampour H, Gilbert BP, Bailleres H. Numerical study on the flexural capacity of ultra-light composite timber sandwich panels. Compos Part B. 2018;155:212–24. https://doi.org/10.1016/j.compositesb.2018.08.022.
42. Darzi S, Karampour H, Bailleres H, Gilbert BP, McGavin RL. Experimental study on bending and shear behaviours of composite timber sandwich panels. Constr Build Mater. 2020;259:119723. https://doi.org/10.1016/j.conbuildmat.2020.119723.
43. Darzi S, Karampour H, Bailleres H, Gilbert BP, Fernando D. Load bearing sandwich timber walls with plywood faces and bamboo core. Structures. 2020;27:2437–50. https://doi.org/10.1016/j.istruc.2020.08.020.
44. Hartoni, J. Fajrin, B. Anshari, A.D. Catur. 2017 Effect of core and skin thicknesses of bamboo sandwich composite on bending strength. Int J Mech Eng Technol. 8 551–560, http://www.iaeme.com/IJMET/issues.asp?JType=IJMET&VType=8&IType=12 Accessed 02 Dec 2020.
45. Oliveira LA, Coura GLC, Tonatto MLP, Panzera TH, Placet V, Scarpa F. A novel sandwich panel made of prepreg flax skins and bamboo core. Compos Part C. 2020;3:100048. https://doi.org/10.1016/j.jcomc.2020.100048.
46. Oliveira LA, Nicholas JO, Freire RTS, Panzera TH, Christoforo AL, Scarpa F. Sustainable sandwich panels made of aluminium skins and bamboo ring. Mater Res. 2021;24:1. https://doi.org/10.1590/1980-5373-mr-2020-0543.
47. Oliveira LA, Tonatto MLP, Coura GLC, Freire RTS, Panzera TH, Scarpa F. Experimental and numerical assessment of sustainable bamboo core sandwich panels under low-velocity impact. Constr Build Mater. 2021;292:123437. https://doi.org/10.1016/j.conbuildmat.2021.123437.
48. ASTM D638-14, Standard Test Method for Tensile Properties of Plastics, ASTM International, West Conshohocken, PA, 2014. https://doi.org/10.1520/D0638-14.

49. ASTM D695-15, Standard Test Method for Compressive Properties of Rigid Plastics, ASTM International, West Conshohocken, PA, 2015. https://doi.org/10.1520/D0695-15.
50. ASTM D790-15, Standard test methods for flexural properties of unreinforced and reinforced plastics and electrical insulating materials, ASTM International, West Conshohocken, PA, 2015. https://doi.org/10.1520/D0790-15.
51. Dessalegn Y, Singh B, van Vuure AW, Rajhi AA, Ahmed GM, Hossain N. Influence of age and harvesting season on the tensile strength of bamboo-fibre-reinforced epoxy composites. Mater. 2022. https://doi.org/10.3390/ma15124144.
52. ASTM E8/E8M-16a, Standard test methods for tension testing of metallic materials, ASTM International, West Conshohocken, PA, 2016. https://doi.org/10.1520/E0008_E0008M-16A.
53. ASTM D3039/3039M-17, Standard test method for tensile properties of polymer matrix composite materials, ASTM International, West Conshohocken, PA, 2017. https://doi.org/10.1520/D3039_D3039M-17.
54. ASTM D792–20, Standard test methods for density and specific gravity (relative density) of plastics by displacement, ASTM International, West Conshohocken, PA, 2020. https://doi.org/10.1520/D0792-20
55. D.C. Montgomery, Design and Analysis of Experiments. John Wiley & Sons. 5th Ed. (2001).
56. Wu W, Abliz D, Jiang B, Ziegmann G, Meiners D. A novel process for cost effective manufacturing of fibre metal laminate with textile reinforced pCBT composites and aluminum alloy. Compos Struct. 2014;108:172–80. https://doi.org/10.1016/j.compstruct.2013.09.016.
57. Li Z, Luan Y, Hu J, Fang C, Liu L, Ma Y, Liu Y, Fei B. Bamboo heat treatments and their effects on bamboo properties. Constr & Build Mater. 2022;331: 127320. https://doi.org/10.1016/j.conbuildmat.2022.127320.
58. Wu X, Fan Z, Wang J, Wang H, Han S, Zhang Y, Sun F. Improving the anti-mould capacity of bamboo through sequential alkaline extraction and laccase-mediated thymol modification. Constr & Build Mater. 2022;354: 129104. https://doi.org/10.1016/j.conbuildmat.2022.129104.
59. ASTM D1002–10, Standard test method for apparent shear strength of single-lap-joint adhesively bonded metal specimens by tension loading (metal-to-metal), ASTM International, West Conshohocken, PA, 2010. https://doi.org/10.1520/D1002-10R19
60. Santana PRT, Panzera TH, Freire RTS, Christoforo AL. Apparent shear strength of hybrid glass fibre reinforced composite joints. Polym Test. 2017;64:307–12. https://doi.org/10.1016/j.polymertesting.2017.10.022.
61. ASTM D5868–01(2014), Standard test method for lap shear adhesion for fibre reinforced plastic (FRP) bonding, ASTM International, West Conshohocken, PA, 2014. https://doi.org/10.1520/D5868-01R14
62. ASTM C393/C393M-16, Standard test method for core shear properties of sandwich constructions by beam flexure, ASTM International, West Conshohocken, PA, 2016. https://doi.org/10.1520/C0393_C0393M-16
63. ASTM D7250/D7250M-16, Standard Test method for determining sandwich beam flexural and shear stiffness, ASTM International, West Conshohocken, PA, 2016. https://doi.org/10.1520/D7250_D7250M-16
64. Allen HG. Analysis and design of structural sandwich panels. In: Neal BG, editor. Sandwich Beams. Amsterdam: Elsevier; 1969.
65. Rejab MRM, Cantwell WJ. The mechanical behaviour of corrugated-core sandwich panels. Compos Part B. 2013;47:267–77. https://doi.org/10.1016/j.compositesb.2012.10.031.
66. Santos JC, Vieira LMG, Panzera TH, Schiavon MA, Christoforo AL, Scarpa F. Hybrid glass fibre reinforced composites with micro and poly-diallyldimethylammonium chloride (PDDA) functionalised nano silica inclusions. Mater Design. 2015;65:543–9. https://doi.org/10.1016/j.matdes.2014.09.052.
67. Ferreira BT, da Silva LS, Panzera TH, Santos JC, Freire RTS, Scarpa F. Sisal-glass hybrid composites reinforced with silica microparticles. Polym Test. 2019;74:57–62. https://doi.org/10.1016/j.polymertesting.2018.12.026.
68. Rudawska A. Adhesive joint strength of hybrid assemblies: titanium sheet-composites and aluminium sheet-composites—Experimental and numerical verification. Int J Adhes Adhes. 2010;20:574–82. https://doi.org/10.1016/j.ijadhadh.2010.05.006.
69. Gottron J, Harries KA, Xu Q. Creep behaviour of bamboo. Constr Build Mater. 2014;66:79–88. https://doi.org/10.1016/j.conbuildmat.2014.05.024.
70. Hu LL, He XL, Wu GP, Yu TX. Dynamic crushing of the circular-celled honeycombs under out-of-plane impact. Int J Impact Eng. 2015;75:150–61. https://doi.org/10.1016/j.ijimpeng.2014.08.008.
71. Akatay A, Bora MO, Fidan S, Coban O. Damage characterisation of three-point bended honeycomb sandwich structures under different temperatures with cone beam computed tomography technique. Polym Composite. 2015;39:46–54. https://doi.org/10.1002/pc.23900.
72. Available https://www.professionalplastics.com/professionalplastics/Gillfab_4030.pdf Accessed 03 May 2021.